Continuous variable entanglement enhancement and manipulation by a subthreshold Type II optical parametric amplifier

Yana Shang, Xiaojun Jia,* Yumei Shen, Changde Xie, and Kunchi Peng

State Key Laboratory of Quantum Optics and Quantum Optics Devices, Institute of Opto-Electronics, Shanxi University, Taiyuan, 030006, China

**Corresponding author: jiaxj@sxu.edu.cn*

Received November 30, 2009; revised January 26, 2010; accepted January 29, 2010; posted February 16, 2010 (Doc. ID 120721); published March 15, 2010

We experimentally demonstrate that the quantum entanglement between amplitude and phase quadratures of optical modes produced from a nondegenerate optical parametric amplifier (NOPA) can be enhanced and manipulated phase sensitively by means of another NOPA. When both NOPAs operate at deamplification, the entanglement degree is increased at the cavity resonance of the second NOPA. When the first NOPA operates at deamplification and the second one at amplification, the spectral features of the correlation variances are significantly changed. The experimental results are in good agreement with the theoretical expectation. © 2010 Optical Society of America

OCIS codes: 270.6570, 190.4410.

The entangled states of light with amplitude and phase quadrature quantum correlations have been extensively applied in continuous variable (CV) quantum information [1–4]. It is significant to enhance and manipulate quantum entanglement of optical entangled states for realizing high-quality information processing and achieving long-distance quantum communication. The phase-sensitive responses of quantum states of light through a degenerate optical parametric amplifier (DOPA) have been theoretically studied by Agarwal [5]. The phase-sensitive manipulation of a squeezed vacuum field in a DOPA [6] and the low-noise phase-insensitive amplification of a CV quantum state [7,8] have been experimentally demonstrated. Besides DOPAs, nonclassical optical fields, such as squeezed states and entangled states, can be directly generated from a continuous Type II nondegenerate optical parametric amplifier (NOPA) operated below and above the oscillation threshold, respectively [3,4,9–11]. Recently, it has been theoretically proved that the entanglement features of Einstein–Podolsky–Rosen (EPR) optical beams can be phase-sensitively manipulated by another NOPA [12]. Here, we present what we believe to be the first experimental demonstration on the phase-sensitive manipulation of EPR entangled states. Two NOPAs are used in the experiment, one for the generation of EPR beams and another one for entanglement manipulating. The quantum entanglement between amplitude and phase quadratures of EPR beams produced from the first NOPA are enhanced when both NOPAs operate at deamplification. When the first NOPA operates at deamplification and the second one at amplification, the spectral features of the correlation variances are significantly changed. The experimental results demonstrate that the quantum correlation features of an optical entangled state can be manipulated by controlling the relative phase between the pump field and the injected fields of the second NOPA, which are in good agreement with the theoretical expectation in [12].

The experimental setup is shown in Fig. 1. A homemade cw frequency-doubled and frequency-stabilized (Nd-dropped $YAlO_3$/$KTiOPO_4$) (Nd:YAP/KTP) laser with both harmonic (540 nm) and subharmonic (1080 nm) outputs serves as the light source for the pump, signal, and local oscillator (LO) [3]. The first NOPA (NOPA1) is in a semimonolithic F-P configuration consisting of an α-cut Type II KTP crystal with 10 mm length and a concave mirror (M0) with 50 mm radius of curvature. The KTP crystal implements the noncritical phase-matching frequency-down-conversion of the pump field [13]. The front face of the crystal is coated to be used as the input coupler (the transmission 95.2% at 540 nm and 0.2% at 1080 nm), M0 serves as the output coupler for the EPR beam at 1080 nm (the transmission of 3.2% at 1080

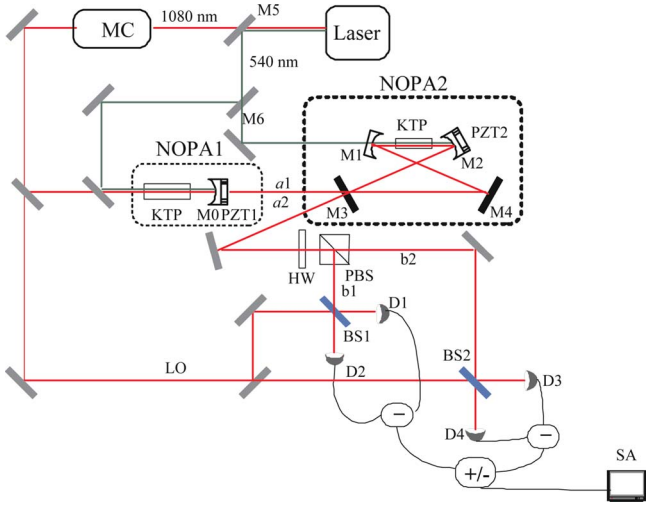

Fig. 1. (Color online) Experimental setup. laser, Nd:YAP/KTP laser source; HW, λ/2 wave plate; PBS, polarizing beam splitter; BS1–BS2, 50/50 beam splitter; D1–D4, ETX500 InGaAs photodiode detectors; +/−, positive/negative power combiner; MC, mode cleaner; M0–M6, different mirrors (see text for details); PZT, piezoelectric transducer; SA, spectrum analyzer.

nm), which is mounted on a piezoelectric transducer (PZT) to scan or lock actively the cavity length as needed. The second NOPA (NOPA2) is in a ring configuration consisting of two concave mirrors with 100 mm radius of curvature (M1 and M2) and two flat mirrors (M3 and M4). An α-cut Type II KTP crystal of 10 mm length with the 1080 and 540 nm dual-band antireflection coated at two end faces is placed at the middle between M1 and M2. M3 serves as the input and the output coupler of light at 1080 nm with the transmission of 3.5% at 1080 nm. The length and the finesse of the cavity for NOPA1 (NOPA2) are 51 mm (557 mm) and 165 (153), respectively. The output signal and idler beams (b_1 and b_2) from NOPA2 are separated by a polarizing beam splitter (PBS), and then they are respectively sent to two balanced homodyne detectors for simultaneously measuring the noise power spectra of their quadrature components. The measured noise powers are combined by a positive or negative power combiner (+/−), and then the combined correlation variances of amplitude or phase quadratures between b_1 and b_2 are detected by a spectrum analyzer (SA).

At first, we achieved the double resonance of an injected subharmonic coherent signal and idler in NOPA1 using the frequency modulation sideband technique [3,13]. Then the relative phase between the pump field and the injected signal field is locked to π, that is to enforce the NOPA1 operating at deamplification [3]. When a block was inserted between M3 and M4 and the pump light of NOPA2 was turned off, the output light by NOPA1 was not coupled into NOPA2 and was almost totally reflected by M3 to PBS. In this case the quadrature correlation variances of the EPR beams produced by NOPA1 were measured. The measured correlation variances spectra of the amplitude sum, $\langle\delta^2(\hat{X}_{a_1}+\hat{X}_{a_2})\rangle$, and the phase difference, $\langle\delta^2(\hat{Y}_{a_1}-\hat{Y}_{a_2})\rangle$, both were 2.4±0.1 dB below the corresponding shot noise limit (SNL) at the analysis frequency of $\Omega=3.0$ MHz, where $\hat{X}_{a_1}$ and $\hat{X}_{a_2}$ ($\hat{Y}_{a_1}$ and $\hat{Y}_{a_2}$) are the amplitude (phase) quadratures of output modes a_1 and a_2 by NOPA1, respectively. It means that the EPR entangled optical field with the amplitude anticorrelation and the phase correlation were obtained. During the experiment the pump power and intensity of the injected signal for NOPA1 are kept at 120 mW (below the oscillation threshold of 200 mW) and 10 mW before the input coupler, respectively. The power of the output EPR entangled beams is about 52 μW.

By removing the block between M3 and M4 as well as turning on the pump light of NOPA2, the EPR beams by NOPA1 were injected into NOPA2. When NOPA2 was operated at deamplification, the output signal and idler modes by NOPA2 were still entangled with the anticorrelation of amplitude quadratures ($\langle\delta^2(\hat{X}_{b_1}+\hat{X}_{b_2})\rangle<$SNL) and the correlation of phase quadratures ($\langle\delta^2(\hat{Y}_{b_1}-\hat{Y}_{b_2})\rangle<$SNL) such as the entanglement features of the injected signals, where $\hat{X}_{b_1}$ and $\hat{X}_{b_2}$ ($\hat{Y}_{b_1}$ and $\hat{Y}_{b_2}$) are the amplitude (phase) quadratures of output modes b_1 and b_2 by the NOPA2, respectively. The correlation variance spectra of $\langle\delta^2(\hat{X}_{b_1}+\hat{X}_{b_2})\rangle$ and $\langle\delta^2(\hat{Y}_{b_1}-\hat{Y}_{b_2})\rangle$ versus the cavity detuning measured by scanning the length of the optical cavity of NOPA2 are shown in Figs. 2(a) and 2(b). Under the resonance with zero detuning ($\Delta=0$), both the variance of the amplitude sum [Fig. 2(a) trace iii] and the phase difference [Fig. 2(b) trace iii] are about 3.0 dB below the SNL (trace i). By locking the cavity length to the resonance point a stable correlation variance of 3.0±0.1 dB below the SNL is obtained (trace iv). In this case the entanglement degree of the output fields by NOPA2 is enhanced about 0.6 dB with respect to that of the injected entangled states. Trace ii in Figs. 2(a) and 2(b) is the correlation variance spectra of the (a) amplitude sum and (b) phase difference calculated by Eq. (25) in [12] with the actual parameters of the experimented system, respectively. Deviating from the resonance with a small detuning the correlation noises increase rapidly to two maximums of 2.0 dB above the SNL at $\Delta=\pm4.9$ MHz and then decrease to the initial correlation degree of the injected EPR beams (~2.4 dB below the SNL) at far detuning.

However, if NOPA2 is operated at amplification by locking the relative phase between the pump field and the injected EPR beam in phase and NOPA1 still at deamplification, the correlation features of quadratures between output modes b_1 and b_2 will be significantly changed. In this case the noise powers of $\langle\delta^2(\hat{X}_{b_1}+\hat{X}_{b_2})\rangle$ and $\langle\delta^2(\hat{Y}_{b_1}-\hat{Y}_{b_2})\rangle$ are not squeezed. In contrast with the correlation features of the injected EPR beams with $\langle\delta^2(\hat{X}_{a_1}+\hat{X}_{a_2})\rangle<$SNL and $\langle\delta^2(\hat{Y}_{a_1}-\hat{Y}_{a_2})\rangle<$SNL, the correlation variances of the output fields by NOPA2, $\langle\delta^2(\hat{X}_{b_1}-\hat{X}_{b_2})\rangle$ and $\langle\delta^2(\hat{Y}_{b_1}+\hat{Y}_{b_2})\rangle$, become the quantum correlated with noise powers below the SNL at the cavity resonance and near reso-

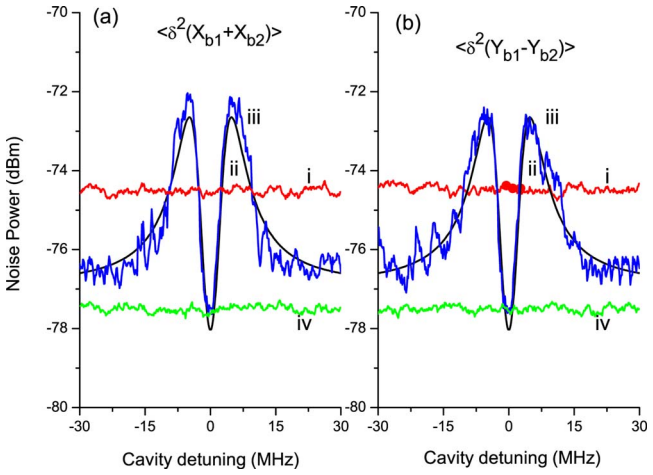

Fig. 2. (Color online) Noise powers of the correlation variances of the output beams from NOPA2 operated at deamplification versus cavity detuning: (a) for amplitude sum $\langle\delta^2(\hat{X}_{b_1}+\hat{X}_{b_2})\rangle$, (b) for phase difference $\langle\delta^2(\hat{Y}_{b_1}-\hat{Y}_{b_2})\rangle$. Trace i, SNL; trace ii, theoretically calculated results; trace iii, measured variance spectrum with the cavity detuning; trace iv, measured variance power with the cavity locked on resonance.

nance. Figures 3(a) and 3(b) are the noise power spectra of $\langle \delta^2(\hat{X}_{b_1} - \hat{X}_{b_2})\rangle$ and $\langle \delta^2(\hat{Y}_{b_1} + \hat{Y}_{b_2})\rangle$ versus the cavity detuning of NOPA2 at $\Omega = 3.0$ MHz. Trace i is the SNL; traces ii and iii are the noise power spectra calculated by Eq. (25) in [12] and experimentally measured, respectively; trace iv is the noise spectra measured when the cavity of NOPA2 is locked at the resonance. Both correlation variances of the (a) amplitude difference and (b) phase sum at the cavity resonance are 0.4 dB below the SNL and the minimal variance of 1.4 dB below the SNL appear at small detuning of $\Delta = \pm 3.5$ MHz. Then, the variances increase to much higher than the SNL at far detuning where the parametric interaction in NOPA2 no longer exists and thus $(\hat{X}_{b_1} - \hat{X}_{b_2})$ and $(\hat{Y}_{b_1} + \hat{Y}_{b_2})$ return to antisqueezing components of the initially injected modes a_1 and a_2.

When NOPA1 and NOPA2 are operated at the same regime (Fig. 2) the identical parametric interaction in NOPA2 will enhance the entanglement of the injected signal field. However, if NOPA1 and NOPA2 are operated at the opposite regime (Fig. 3), the quantum correlations produced by the nonlinear process in NOPA2 have the opposite features with the correlations of the injected signal field at the resonance and the near resonance. Thus the amplitude anticorrelation and the phase correlation of the injected field are changed to the amplitude correlation and the phase anticorrelation of the output field due to the parametric amplification process in NOPA2. The shoulders appearing in the spectral shapes just outside the resonant point are caused by the interference between the pump field and the subharmonic seed field in NOPA2 in cooperation with the absorptive and dispersive responses of an optical cavity [12]. Comparing traces ii and iii in Figs. 2 and 3, we can see that theoretically calculated and experimentally measured correlation variance spectra are in good agreement except at the dips of the minimal variances. At these dips the calculated variances are smaller than the measured values, which is perhaps because some extra instability appears at the suddenly changing points of the correlation variances that have not been involved in the theoretical equations.

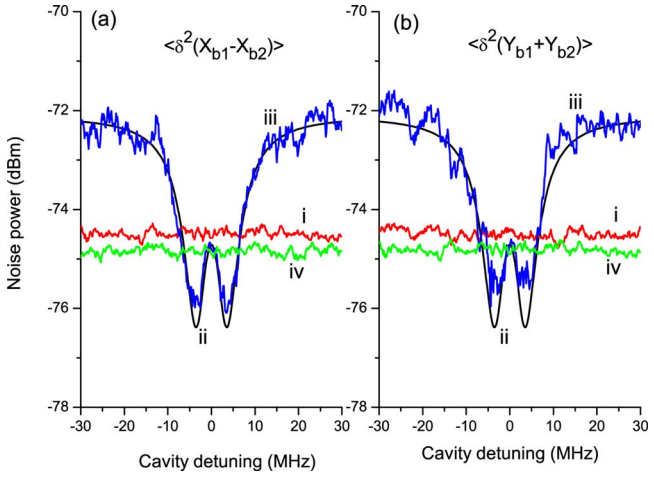

Fig. 3. (Color online) Noise powers of the correlation variances of the output beams from NOPA2 operated at amplification versus cavity detuning: (a) for amplitude difference $\langle \delta^2(\hat{X}_{b_1} - \hat{X}_{b_2})\rangle$, (b) for phase sum $\langle \delta^2(\hat{Y}_{b_1} + \hat{Y}_{b_2})\rangle$. Trace i, SNL; trace ii, theoretically calculated results; trace iii, measured variance spectrum with the cavity detuning; trace iv, measured variance power with the cavity locked on resonance.

In conclusion, we experimentally realized the entanglement enhancement and phase-sensitive manipulation of CV optical entangled states based on using NOPAs. The experiment provides a simple scheme to increase and manipulate CV quantum correlations of optical modes without the need for the difficult technique of single photon detection [14].

This research was supported by the National Natural Science Foundation of China (NSFC) (grants No. 60736040 and No. 60608012), NSFC Project for Excellent Research Team (grant No. 60821004), and National Basic Research Program of China (grant No. 2010CB923103).

References

1. S. L. Braunstein and P. van Loock, Rev. Mod. Phys. **77**, 513 (2005).
2. M. D. Reid, P. D. Drummond, W. P. Bowen, E. G. Cavalcanti, P. K. Lam, H. A. Bachor, U. L. Andersen, and G. Leuchs, Rev. Mod. Phys. **81**, 1727 (2009).
3. X. Y. Li, Q. Pan, J. T. Jing, J. Zhang, C. D. Xie, and K. C. Peng, Phys. Rev. Lett. **88**, 047904 (2002).
4. V. D'Auria, S. Fornaro, A. Porzio, S. Solimeno, S. Olivares, and M. G. A. Paris, Phys. Rev. Lett. **102**, 020502 (2009).
5. G. S. Agarwal, Phys. Rev. Lett. **97**, 023601 (2006).
6. J. Zhang, C. G. Ye, F. Gao, and M. Xiao, Phys. Rev. Lett. **101**, 233602 (2008).
7. U. L. Andersen, V. Josse, and G. Leuchs, Phys. Rev. Lett. **94**, 240503 (2005).
8. R. C. Pooser, A. M. Marino, V. Boyer, K. M. Jones, and P. D. Lett, Phys. Rev. Lett. **103**, 010501 (2009).
9. A. S. Villar, L. S. Cruz, K. N. Cassemiro, M. Martinelli, and P. Nussenzveig, Phys. Rev. Lett. **95**, 243603 (2005).
10. J. T. Jing, S. Feng, R. Bloomer, and O. Pfister, Phys. Rev. A **74**, 041804 (2006).
11. G. Keller, V. D'Auria, N. Treps, T. Coudreau, J. Laurat, and C. Fabre, Opt. Express **16**, 9351 (2008).
12. H. X. Chen and J. Zhang, Phys. Rev. A **79**, 063826 (2009).
13. Z. Y. Ou, S. F. Pereira, H. J. Kimble, and K. C. Peng, Phys. Rev. Lett. **68**, 3663 (1992).
14. A. Ourjoumtsev, A. Dantan, R. Tualle-Brouri, and P. Grangier, Phys. Rev. Lett. **98**, 030502 (2007).